CW-OPO based cavity-leak-out spectrometer for ultra-sensitive and selective mid infrared trace gas analysis

Frank Kühnemann[a,c], Frank Müller[a,d], Golo von Basum[b], Daniel Halmer[b], Alexander Popp[a], Stephan Schiller[d], Peter Hering[b], Manfred Mürtz[b],

[a]Institute of Applied Physics, Bonn University, Wegelerstrasse 8, D-53115 Bonn, Germany;

[b]Institute of Laser Medicine, Düsseldorf University, Universitätsstrasse 1, D-40225 Düsseldorf, Germany;

[c]Max Planck Institute of Chemical Ecology, Hans-Knöll-Strasse 8, D-07745 Jena, Germany;

[d]Institute of Experimental Physics, Düsseldorf University, Universitätsstrasse 1, D-40225 Düsseldorf, Germany

ABSTRACT

An all-solid-state infrared trace gas sensor is presented combining a continuous-wave optical parametric oscillator (OPO) with Cavity Leak-Out spectroscopy (CALOS), a cw version of Cavity Ring Down spectroscopy. The PPLN based pump resonant, singly resonant OPO is pumped at 1064 nm (2 W). Dual cavity design allows to select any desired wavelength within the emission range of the OPO (3.1 - 3.8 μm) and to use different tuning schemes in order to scan absorption features. To detect the CALOS signals the OPO frequency is scanned over the cavity resonance at kHz rates. The high power of the OPO (up to 100 mW at each end of the cavity) allows a strong excitation of the TEM_{00} mode of the cavity, yielding large detector signals. A noise-equivalent absorption coefficient of $1.6 \cdot 10^{-10}\mathrm{cm}^{-1}/\sqrt{\mathrm{Hz}}$ is reached for integration times up to 180 sec. This corresponds to a detection limit for ethane at sub-ppt level. Measurements at reduced pressure (100 mbar) combined with a scanning of the OPO over cm^{-1} wide regions allows a multi-gas analysis of ambient air and human breath samples without a cooling-trap.

Keywords: optical parametric oscillator, nonlinear optics, all-solid-state lasers, mid infrared spectroscopy, trace gas analysis

1. INTRODUCTION

The detection of trace gases is of high importance in a number of fields, such as environmental monitoring, medical breath analysis, food quality control, detection of explosives, purity control for semiconductor process gases or the regulation of combustion processes. As different as the applications are the selected techniques, depending on the required sensitivity, the matrix conditions, the time resolution and other conditions. A particularly challenging field are mobile analyzers which combine high sensitivity, selectivity and speed. When spectroscopic detection methods are considered, infrared techniques are favorable for the monitoring of molecular species at the parts-per-billion (ppb, mixing ratio $1{:}10^{-9}$) level and below, as they frequently occur in environmental applications, medical or biological studies. Several techniques have been reported to provide such detection sensitivities, such as photoacoustic spectroscopy,[1,2] Faraday modulation spectroscopy,[3] cavity ring-down spectroscopy[4] (CRDS) or cavity leak-out spectroscopy (CALOS) which is a cw version of CRDS.[5] The development of mobile detection systems strongly depends on the availability of suitable all solid state mid-infrared laser light sources, which have to provide tunability, wavelength stability, possible modulation schemes and a power level which meet the requirements of the respective detection method. During the last years a number of new sources has been developed and applied for spectroscopy and detection in the mid-infrared, namely difference frequency generation (DFG),[6] optical parametric oscillators (OPO)[2] and quantum cascade lasers (QCL).[7]

Send correspondence to F.K.: e-mail: kuehnemann@iap.uni-bonn.de, phone: +49 228 733453

A growing field for applications is the detection of light hydrocarbons and other organic molecules at sub-ppb concentrations which are of particular importance in biochemical and physiological processes both in plant biology and medicine. Suitable devices shall allow to monitor the emission of such volatile compounds by living organisms form single cells to plants, animals and men, thus yielding valuable information on physiological or developmental processes in a non-invasive way. Examples for this are the emission of ethylene (a plant hormone and stress indicator)[8] and ethane (produced upon lipid peroxidation)[9] by green plants. In medicine, a number of compounds found in the breath are considered to be markers for stress situations or diseases, such as ethane (increased oxidative stress),[10] acetone (as an indicator for diabetes),[11] isoprene (biochemical stress).[12]
In this paper we present our results of the development of a cw OPO based CALOS spectrometer operating in the 3 μm region and its application to acetone and ethane detection. The tuning properties of a dual cavity OPO based on periodically poled lithium niobate combined with the careful implementation of data acquisition and analysis allowed us to improve the detection limits and selectivity considerably.

2. OPTICAL PARAMETRIC OSCILLATOR

The continuously pumped optical parametric oscillator is based on periodically poled lithium niobate (PPLN). It is set up it a dual-cavity design for pump and signal resonance (dc-PR-SRO).[13] The PPLN crystal (19 mm long) contains 19 gratings with poling periods between 28.64 μm and 30.16 μm and is mounted inside a self designed oven for operation at temperatures between 150 and 200 deg C. The temperature stability is 8 mK (standard deviation) over 4 hours. The first crystal surface is HR coated for both pump (94.3 %) and signal (99.9 %) waves thus serving as the common first mirror for both resonators. The pump-cavity (FSR $\sim$ 2.7 GHz) is closed by a meniscus mirror (r_{cav} = 30 mm, r_{vex} = 15 mm) with 99.9 % pump reflection. This mirror is AR coated for both signal and idler (AR $<$ 2 % for signal and AR $<$ 5 % for idler). The second (signal) cavity with a FSR of 450 MHz is closed by a concave mirror (r_{cav} = 450 mm, HR 99.9 % reflectivity for signal, $<$ 5 % for idler). Both mirrors are mounted on piezoelectric transducers (PZT). A galvanometer-mounted etalon (YAG, 0.5 mm, $\sim$ 50 % signal reflectivity coating) is inserted into the signal cavity to suppress spontaneous mode-hops. The pump beam is focused (r_{waist} = 34 μm) at the front face of the PPLN crystal with a lens (f = 100 mm). The pump enhancement lowers the external pump threshold down to 380 mW. Using a 2.5 Watt Nd:YAG pump laser (1064

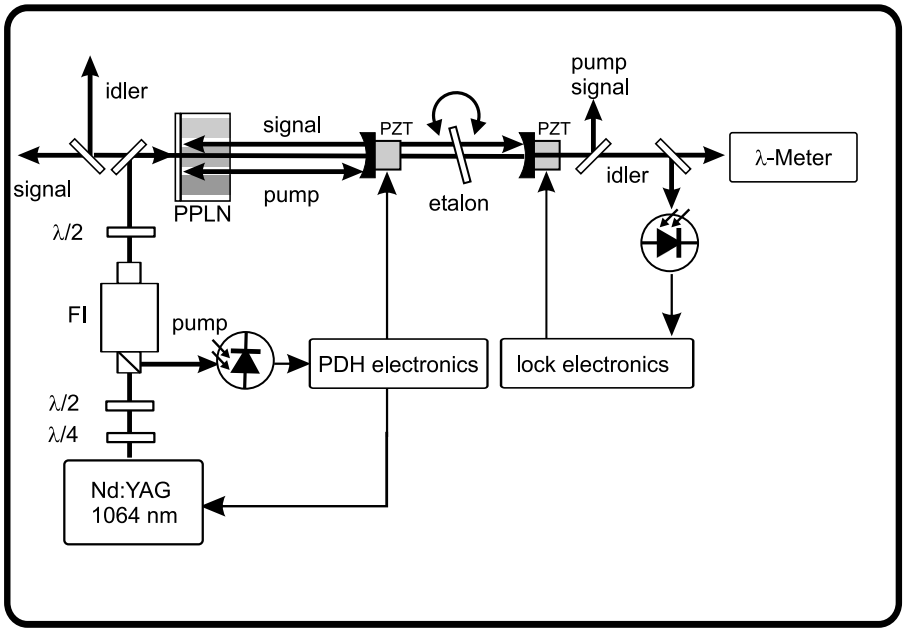

Figure 1: Setup of the cw dual-cavity Optical parametric oscillator. Indicated are the lock circuits for the pump cavity and the signal cavity stabilization. PPLN: periodically poled lithium niobate, FI: Faraday isolator, PZT: piezo-ceramic transducer, PDH: Pound-Drever-Hall

nm, Innolight Mephisto, linewidth ~ 1 kHz / 100 msec, frequency drift ~ 1 MHz / min) a maximum idler output power of 2 x 100 mW is achieved, leaving the cavity at both ends. The pump cavity is locked to the laser via the Pound-Drever-Hall (PDH) method. The signal cavity can be locked (using a dither on the signal cavity PZT) to the point of maximum idler power. Mode-hop-free operation is then achieved over typically 45 minutes. During this time the idler frequency drift was below 30 MHz (digital resolution of the WA 1500 wavemeter (Burleigh). With the signal cavity not actively controlled, its length slowly drifts, resulting in mode-hops every 5-10 minutes. The major goal of the development of the *dual-cavity* OPO was the improvement of the idler frequency tuning possibilities in comparison to the *common-cavity* setup.[14] Coarse tuning within the 3.1-3.9 μm operation range is performed by selecting one of the 19 QPM gratings via motor driven translation stage and temperature tuning of the PPLN crystal within the operation range. An example is shown in fig. 2 (left), where the measured idler wavenumber as a function of the crystal temperature is compared to the ethane absorption spectrum in the 3 μm region. The line is a fit to the data based on the temperature dependence of the phase-matching conditions in the PPLN grating. There are several options for frequency tuning combining etalon, signal cavity and pump frequency tuning. The selection of the tuning mode depends on the width of the absorption feature to be scanned or used for trace gas detection, reaching from 150 MHz (individual Doppler-broadened lines at a few mbar) up to 50 GHz for pressure broadened structures at atmospheric pressure consisting of many overlapping lines. Mode hop tuning in steps of 450 MHz by turning the etalon via the galvanometer is sufficient for scanning molecular absorption structures at atmospheric pressure. It can be performed over a range of 52 GHz without significant loss of idler output power. If needed, fast continuous fine tuning over 450 MHz is reached by changing the signal cavity length via a piezoelectric transducer. Setting a new frequency within the 52 GHz etalon working range requires a few seconds and is limited by the refresh rate of the wavemeter and the iteration steps needed.

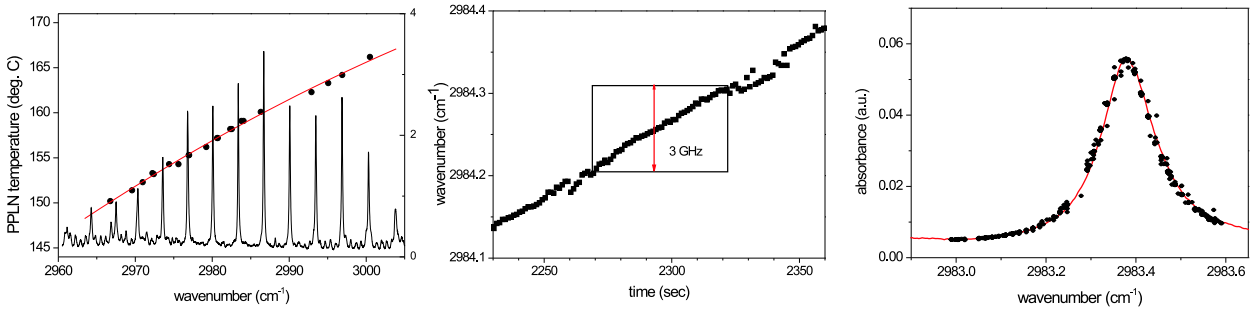

Figure 2: Tuning modes of the dual cavity OPO. *Left*: Temperature tuning of the idler emission. The measured idler wavenumber (dots) are compared to the ethane absorption spectrum in the 3 μm region. *Middle*: Continuous pump tuning. The mode-hop-free tuning range indicated by the box comprises a range of 3 GHz. *Right*: Scan across a single ethane absorption peak at atmospheric pressure through combined etalon-mode-hop tuning and signal cavity tuning.

Additional tuning possibilities arise from the tuning of the pump laser. When the signal frequency is fixed by the intra-cavity etalon, the idler frequency is tuned by the same amount as the pump frequency.[15] Although the gain curve shifts when the pump frequency is tuned, the magnitude of this shift (~ 35 GHz) and the width of the gain curve (several 100 GHz) are such that the spectral line shape of the etalon (FWHM ~ 37 GHz) is the dominant effect, thus preventing signal mode-hops.[16] Mode-hop-free idler tuning over the mode-hop-free tuning range of the laser (9 GHz) should be possible. Until now a tuning range up to 3 GHz is achieved in this tuning mode (Fig. 2, middle). Small structures in the gain curve, possibly due to the optical coatings, may be limiting this range. An extension of the continuous tuning range should be possible by a combined tuning of etalon and signal cavity length.
A modulation of the signal cavity length allows us to implement a frequency modulation of the signal and idler waves up to kHz rates and modulation depths greater than 200 MHz without influencing pump cavity stabilization.

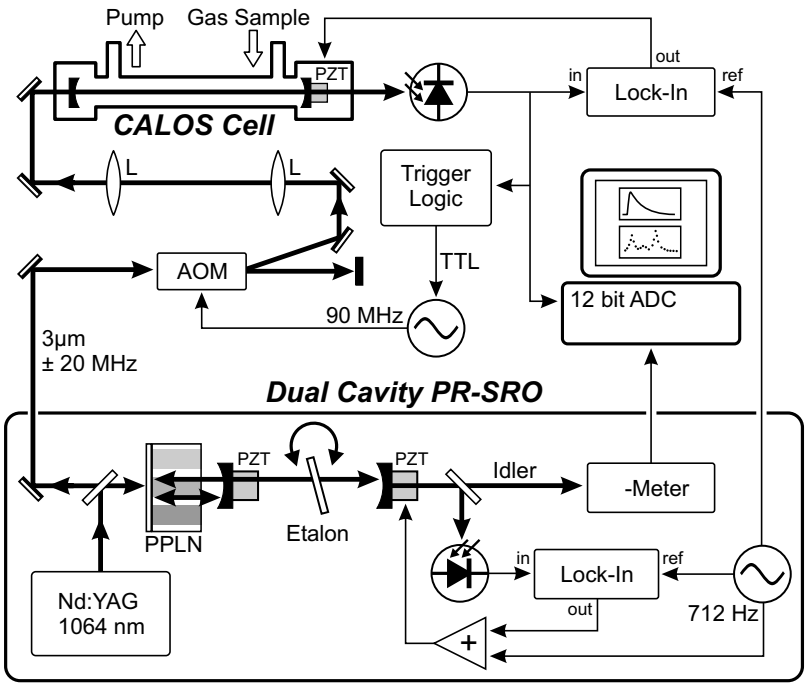

Figure 3: Setup of the OPOCALOS spectrometer. PPLN: periodically poled Lithium niobate, AOM: acousto-optic modulator, PZT: piezo-ceramic transducer, L:lens, PD: photodetector. The OPO stabilization loops are not shown here.

3. CAVITY LEAK OUT SPECTROSCOPY

The complete spectrometer consists of the cw OPO, an acousto-optic modulator (AOM), the absorption cell (CALOS cell) and a fast photodetector. A schematic setup is shown in fig. 3. The CALOS cell is a high finesse optical resonator (L=52.5 cm) formed by two highly reflective mirrors (R = 99.985 %, Los Gatos) as previously described by Kleine et al.[17] The FSR of the cavity is 288 MHz, and the ring-down time for the empty cell is $\sim$11.5 μs. The idler radiation of the OPO is sent through the AOM (Germanium) which is used a s a fast ($< 1\mu s$) switch. The deflected beam is frequency shifted by 90MHz. It is mode matched to the TEM_{00} mode of the CALOS cell by means of two lenses. In order to excite the CALOS cavity the idler frequency of the OPO is

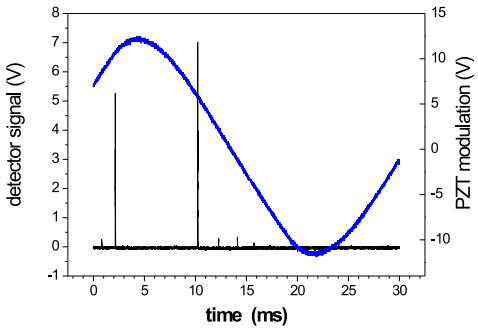

Figure 4: Scanning the idler frequency across the modes of the CALOS cavity. The sinusoidal curve shows the voltage applied to the OPO signal cavity.

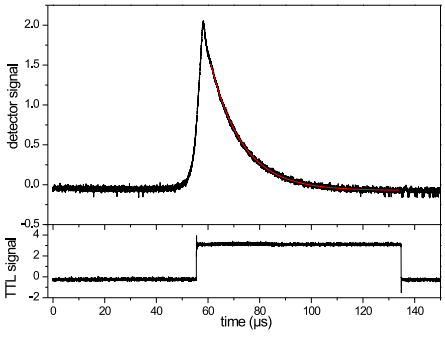

Figure 5: Single ring-down event. The lower trace shows the TTL signal switching off the AOM

periodically modulated through a modulation of the signal cavity length.

A slow scan (fig.4) shows the very good contrast between the TEM_{00} mode and higher modes when the idler frequency is swept periodically. When the transmitted intensity exceeds a certain threshold, a trigger pulse is released, which shuts off the AOM. The subsequent decay of the cavity field is monitored via the photodetector and transferred to a 12-bit analog-to-digital converter card in the control computer. Fig. 5 shows a single decay signal together with the switch signal for the AOM. The decay time of the leak-out signal is determined by fitting a single exponential to the data.

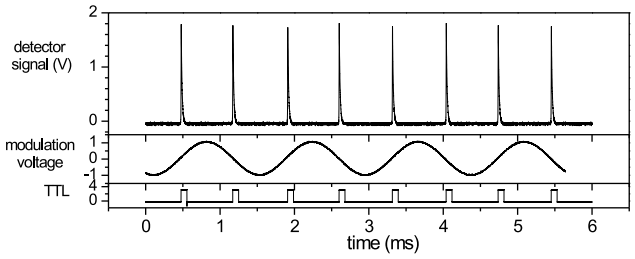

Figure 6: Sequence of Ring-down signals as acquired through modulation of the OPO idler freqency. Upper trace: Detector signal. Middle trace: modulation voltage to the OPO signal cavity. Lower trace: TTL signal to the AOM

A newly developed fast exponential fitting routine (1536 data points within 150 μs.[18]) allows us to analyze every ring-down event individually. The modulation frequency of the idler frequency was increased to 712 Hz, yielding a data acquisition rate of 1.4 kHz, as shown in fig. 6. The modulation depth of the idler frequency is set to approx. 20 MHz to ensure a coincidence between the idler frequency and the CALOS cell resonance in every modulation period, even if drifts of the central idler frequency occur. In addition the length of the CALOS cavity is locked to the idler frequency. Although the idler frequency is tuned across the CALOS cell resonance (approx. 18 kHz wide) in much less than a time constant, the high OPO output power ensures a sufficient excitation of the cavity resonance, thus guaranteeing a strong detector signal in the ring-down phase. This allows fitting of the ring-down signal with high accuracy.
By measuring the decay time of the empty cell (τ_0) as well as the decay time of the cell filled with the gas sample (τ), the absolute absorption coefficient (α) can be determined by

$$\alpha = \frac{1}{c}\left(\frac{1}{\tau} - \frac{1}{\tau_0}\right), \tag{1}$$

where c is the speed of light. The pivotal point for a low detectable absorption coefficient is the accuracy of the ring down time measurement. τ_0 is determined with the CALOS cell filled with grade 5 nitrogen. The results are given in fig. 7, showing the data for the idler wavenumber (upper trace) and the ring-down time τ_0 over a measurement time of 16 minutes. Each data point in the lower trace is the mean of 200 decay times. The step-like shape of the wavenumber data is due to the 30-MHz resolution of the wavemeter. The line represents a running average corresponding to an integration time of 1 s giving a better view at the temporal behaviour of the emission frequency. The ring-down time τ_0 shows a smooth behaviour over periods up to 3 minutes with a rms of about 0.02 %, and jumps in τ_0 correlate with changes in the OPO idler frequency as indicated by the steps in the running average. Within such periods the minimum detectable absorption coefficient is given by the standard error of the mean value, which is $\sigma_{\mathrm{m}} = 1.6 \times 10^{-10}$ cm$^{-1}/\sqrt{\mathrm{Hz}}$. Averaging over up to 180 s results in a noise equivalent absorption of 1.2×10^{-11} cm^{-1}.

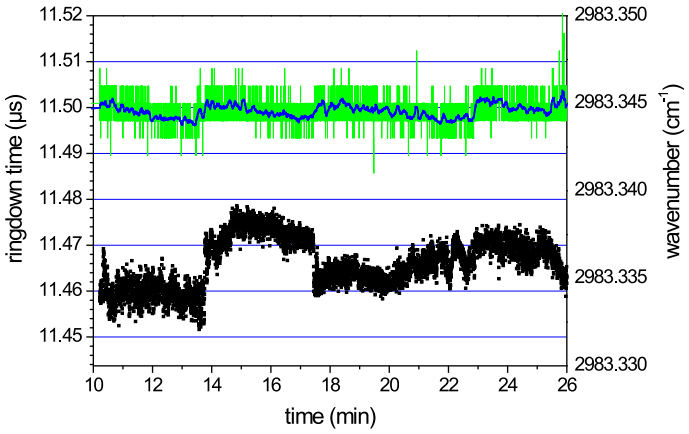

Figure 7: Background signal. Lower trace: ring-down times for the cell filled with grade 5 nitrogen. Upper trace: reading of the wave-meter (30 MHz resolution) and a running average.

3.1. Gas setup

A schematic setup is shown in fig. 8. The ring-down cell is made of stainless steel and has two detachable end pieces. The gas is injected in the middle and extracted at both sides of the absorption cell. The gas flow is maintained by a rotary pump behind the absorption cell. A combination of pressure gage and flow controller ensures a constant gas pressure in the ring-down cell which may range from several mbar to atmospheric pressure. All parts of the gas system are made of glass, stainless steel, or teflon to avoid any contamination with outgassing materials and to reduce possible adsorption effects on the gas sample.

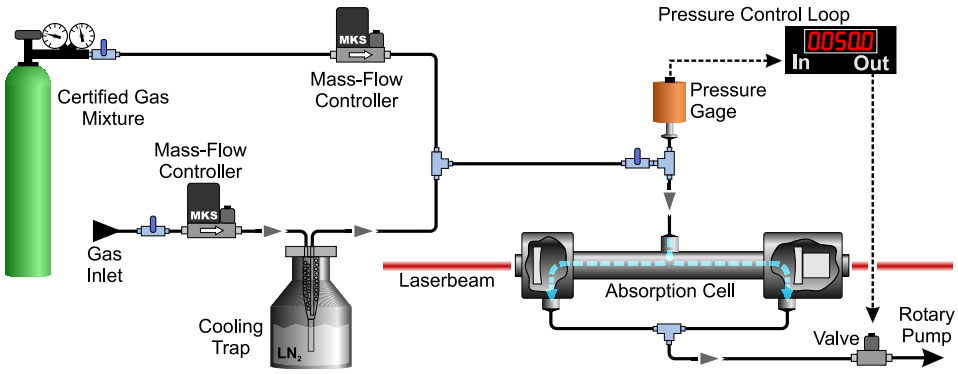

Figure 8: Setup of the gas flow system for calibration and detection measurements

4. APPLICATION

4.1. Acetone detection

Detection of acetone is particularly interesting for the analysis of breath samples in medicine, since it is known to be an indicator for diabetes.[11] Acetone shows a strong absorption peak in the 3 μm range with a characteristic Q branch around 2970 cm^{-1}, which might be used to unambiguously identify acetone in air samples and determine its concentration. This peak is easily reached tuning the OPO at the right frequency. Fig. 9 shows the band and in the insert the mode-hop tuning over parts of the Q branch at a total pressure of 500 mbar. In the insert the FTIR spectrum was scaled to match the CALOS data. (A complete coverage of the peak was prohibited by pump laser problems at the time of the acetone measurements.)

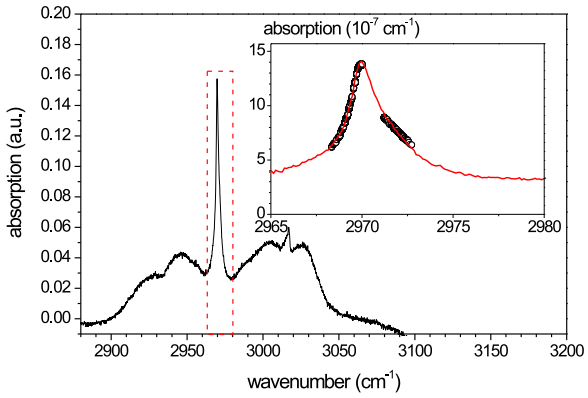

Figure 9: FTIR spectrum of the acetone absorption band around 3 μm. The insert shows an enlarged view of the central Q branch with the data measured with mode-hop tuning of the OPO (open circles).

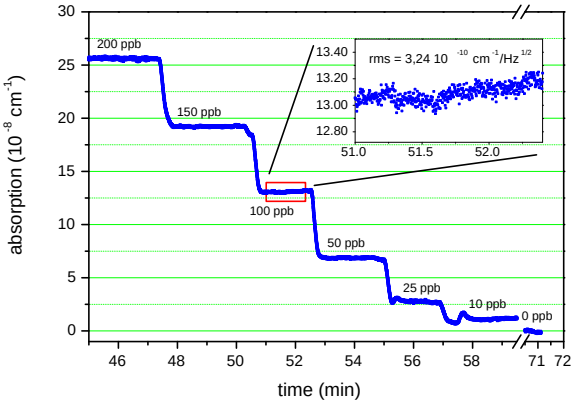

Figure 10: Measured absorption coefficient as a function of the acetone concentration in N_2. The inset demonstrates the noise amplitude (see text).

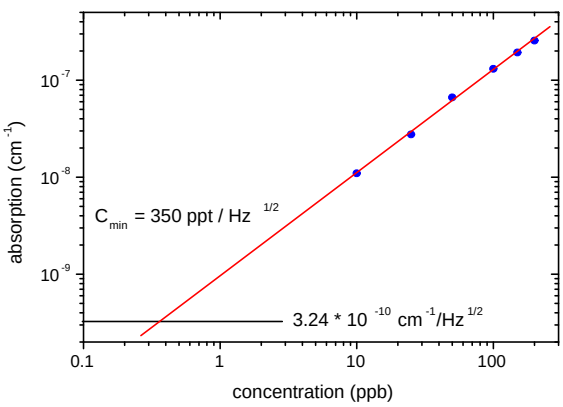

Figure 11: Measured absorption coefficient at the peak of the acetone Q branch as a function of the acetone concentration at a total pressure of 500 mbar.

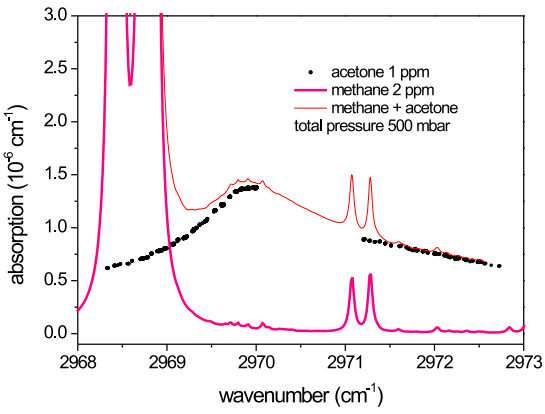

Figure 12: Acetone spectrum: cross interference by methane. The measured spectrum of 1ppm acetone (in N_2) is compared to the simulated spectrum of 2 ppm methane.

In order to determine the sensitivity and detection limit for acetone, a certified mixture of acetone in nitrogen was diluted in several steps (fig. 10). The fluctuation of the signal (as shown in the inset) yields a noise equivalent detection limit of $3.24{\cdot}10^{-10}\mathrm{cm}^{-1}/\sqrt{\mathrm{Hz}}$, which is equivalent to an acetone concentration of 350 ppt/$\sqrt{\mathrm{Hz}}$. The detection of acetone in air samples requires a careful consideration of possible cross interferences due to other compounds. Water vapor is easily removed from the gas flow with a cooling trap at temperatures which do not reduce the acetone concentration. The absorption in the region of the strong Q branch of acetone is, however, strongly influenced by neighboring methane lines. To illustrate this situation fig. 12 shows a simulation for this region. The spectrum of 1 ppm acetone peak (data from the measurement as in fig. 9) is overlaid with the calculated spectrum of methane as derived from the Hitran data base[19] at the ambient concentration of 2 ppm. The upper thin line gives the calculated sum spectrum. The data illustrate that while at 1 ppm the acetone peak is still visible against the methane background, a detection at low ppb levels will not be possible in air containing methane at ambient concentrations. The situation may be improved, however, when acetone detection is to be carried out in the monitoring of trace gas emission by green plants: In such cases it is the standard procedure to supply hydrocarbon-free air to the plant under study thus strongly reducing the risk of methane cross interference.

4.2. Ethane detection

Ethane is an important marker molecule in both medicine and plant biology. It is known to be produced by any kind of tissue as the result of the lipid peroxidation of cell membranes, as it occurs under oxidative stress conditions. A detection limit well below 1 ppb is required, however, if ethane in the human breath is to be used as an early indicator for oxidative stress. This places very high requirements to any technique to be used for the monitoring. Until now the lowest detection limit for ethane had been achieved using photoacoustic spectroscopy with a multi-watt OPO at 3 μm reaching 10 ppt with a 40 seconds integration time.[1]
The strongest ethane absorption peak can be found at 2983.38 cm^{-1}. It consists of a large number of closely spaced absorption lines belonging to the ${}^{p}\mathrm{Q}_1$ subbranch. Figure 13 shows a CALOS scan over this peak using a combination of mode-hop and signal cavity tuning of the OPO idler frequency. The spectrum was recorded with 100 ppb ethane in nitrogen at a total pressure of 100 mbar. For comparison an appropriately scaled FTIR spectrum is given. To derive the ethane sensitivity the CALOS signal was measured at the center of the peak (2983.38 cm^{-1}) for a series of different ethane concentrations. Using two mass-flow controllers a certified gas

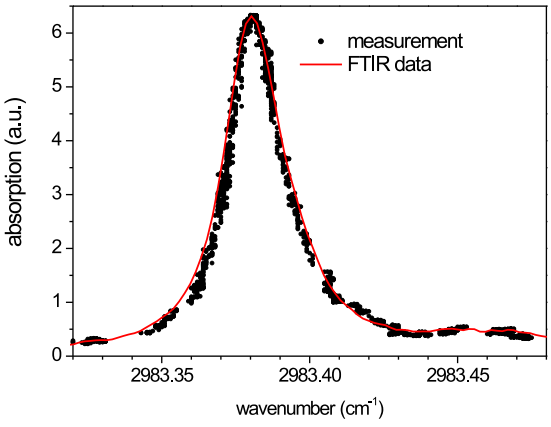

Figure 13: Scan over the ${}^{p}\mathrm{Q}_1$ subbranch of ethane at a total pressure of 100 mbar through combined mode-hop and signal-cavity tuning of the OPO

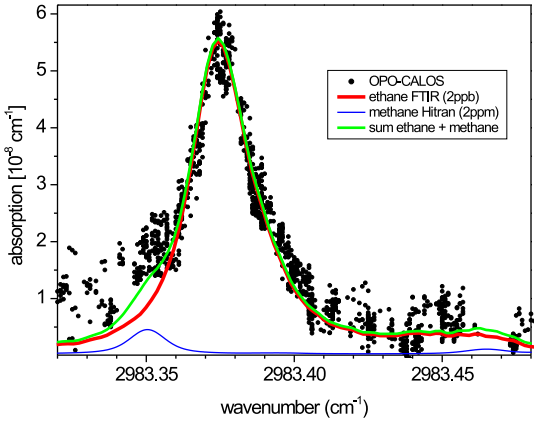

Figure 14: Analysis of an air sample containing about 2 ppb ethane and 2 ppm methane. The curves are the FTIR (ethane) and Hitran (methane) data scaled to match the measured absorption coefficients

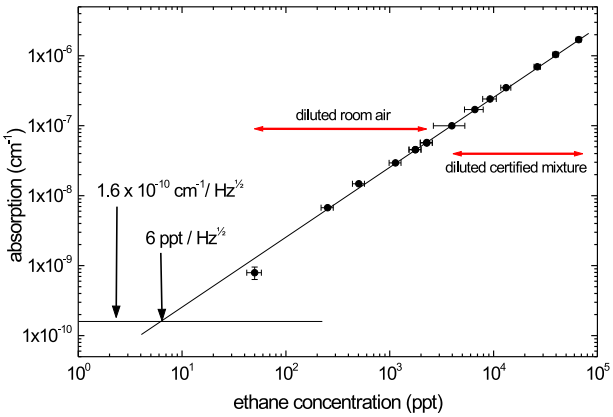

Figure 15: Measured absorption coefficient as a function of ethane concentration using a certified mixture (1 ppm) and room air, as indicated. The line trough the data points is a linear fit.

mixture of ethane in nitrogen (990 ± 50 ppb) was diluted with grade 5 nitrogen to obtain concentrations between 100 ppb and 4 ppb where the lower limit was set by the absolute error of the mass flow controller.
In air samples other molecules besides ethane are present, which might interfere with the ethane detection. The strong ethane absorption peak at 2983.38 cm^{-1} would be hidden under the wing of water absorption lines located at 2983.31 and 2984.21 cm^{-1}. The water is efficiently removed using a liquid nitrogen cooling trap operated at 115 K. Fig. 14 shows an example for the analysis of laboratory air at the strong ethane absorption peak. Under these conditions only a weak methane line is left near the ethane structure and the ethane concentration (2.0±0.2 ppb) is determined by fitting the ethane spectrum (FTIR data) and the methane spectrum (Hitran) to the measured absorption coefficients. Such laboratory air with a known ethane concentration was then used to prepare mixture in the range between 2 and 0.04 ppb through dilution with grade 5 nitrogen. Fig. 15 shows the measured absorption coefficient vs. the concentration for both data sets. The horizontal line in the graph represents the noise level of the current setup as described in the previous section. Its intersection with the slope of the calibration curve reveals a detection limit (SNR = 1) for ethane of 6 ppt/$\sqrt{\text{Hz}}$, which is a factor of 10 better than the previous limits.[1]
Having in mind potential applications it would be even more interesting, if a detection of ethane at ppb and sub-ppb level would be possible without a cooling trap. In this case water vapor and any other volatile compounds absorbing in this region will reach the CALOS cell. The frequency tunability of the OPO allows us to select spectral regions which feature reduced interference by water vapor absorption compared to the peak at 2983.38 cm^{-1}. In the range between 2996.5 and 2997.4 cm^{-1} the spectral data bases show strong and well isolated absorption structures belonging to ethane, methane and water vapor. Figure 16 shows a scan of a laboratory air sample without a cooling trap. Three absorption peaks from ethane, methane and water are visible, whereas

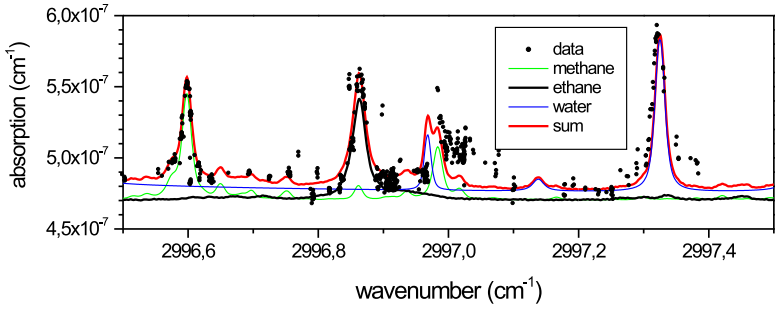

Figure 16: Analysis of an air sample without cooling trap. The lines represent the absorption spectra of ethane, methane and water vapor scaled according to the results of the fit, and the simulated sum compared to the experimental data points.

peaks from other gases are not observed. The measured spectrum shows a strong background ($\sim 4.7{\cdot}10^{-7}\mathrm{cm}^{-1}$) which is about 30 times larger than for a scan of the same region with cooling trap ($\sim 1.4{\cdot}10^{-8}\mathrm{cm}^{-1}$, data not shown here). This background signal is mostly due to the absorption by larger molecules present in the air which show a spectrally flat absorption spectrum in this range and has little influence on the determination of ethane, methane and water vapor. Their concentrations are derived using a linear least squares fit to the data using the Hitran spectra for methane and water vapor and the FTIR spectrum for ethane. The analyzed air sample contained 3.1 ppb ethane, 1.1 ppm methane and 0.36 % water vapor.

5. SUMMARY

We reported on a Cavity Leak Out spectrometer operated with a dual-cavity OPO as the mid-infrared cw light source. The enhanced frequency tunability together with improvements of the data acquisition and processing allows to achieve a detection limit for ethane which is about an order of magnitude lower than previously reported data. The tuning of the OPO allows a simultaneous detection of ethane, methane and water vapor in air samples, even without a cooling trap or any other pre-treatment. The reported setup has the potential for a transportable, all-solid-state, ultra-sensitive trace gas analyzer for environmental and medical studies.
This work was part of the Ph.D. theses of G.v.B and F.M.

REFERENCES

1. M. van Herpen, S.C.Li, S.E.Bisson, and F. Harren, "Photoacoustic trace gas detection of ethane using a continuously tunable, countinous-wave optical parametric oscillator based on periodically poled lithium niobate," *Appl. Phys. Lett.* **81**, p. 1157, 2002.
2. F. Kühnemann, K. Schneider, A. Hecker, A. Martis, W. Urban, S. Schiller, and J. Mlynek, "Photoacoustic trace gas detection using a cw single-frequency parametric oscillator," *Appl. Phys. B.* **66**, pp. 741–745, 1998.
3. H. Ganser, W. Urban, and A. M. Brown, "The sensitive detection of NO by faraday modulation spectroscopy with a quantum cascade laser," *Molecular Physics* **101**, pp. 545–550, 2003.
4. J.J.Scherer, D. Voelkel, D. Rakestraw, J. Paul, C.P.Colier, R. Saykally, and A. O'Keefe, "Infrared cavity ringdown laser absorption spectrosocpy (IR-CLAS)," *Chem. Phys. Lett.* **245**, pp. 273–280, 1995.
5. D. Romanini, A. Kachanov, N. Sadeghi, and F. Stoeckel, "CW cavity ring down spectroscopy," *Chem. Phys. Lett.* **264**, pp. 316–322, 1997.
6. D. Richter, A. Fried, B. Wert, J. Walega, and F. Tittel, "Development of a tunable mid-IR difference - frequency laser source for highly-sensitive airborne trace gas detection," *Appl. Phys. B* **75**, pp. 281–288, 2002.
7. B. Paldus, C. Harb, T. Spence, R. Zare, C. Gmachl, F. Capasso, D. Sivco, J. Baillargeon, A. Hutchinson, and A. Cho, "Cavity ringdown spectroscopy using mid-infrared qunatum cascade lasers," *Opt. Lett.* **25**, pp. 666–668, 2000.
8. F. Abeles, P. Morgan, and J. M.E. Saltveit, *Ethylene in Plant Biology*, Academic Press, San Diego, second ed., 1992.
9. E. Elstner and J. Konze, "Effects of point freezing on ethylene and ethane production by sugar beet leaf disks," *Nature* **263**, pp. 351–352, 1976.
10. M. Knutson, G. Handelman, and F. Viteri, "Methods for measuring ethane and pentane in expired air from rats and humans," *Free Radical Biology & Medicine* **28**, pp. 514–519, 2000.
11. A. Manolis, "The diagnostic potential of breath analysis," *Clin. Chem.* **29**, pp. 5–15, 1983.
12. S. Mendis, P. Sobotka, and D. Euler, "Expired hydrocarbons in patients with acute myocardial infarction," *Free Radic. Res.* **23**, pp. 117–122, 1995.
13. F. Müller, A. Popp, F. Kühnemann, and S. Schiller, "Transportable, highly sensitive photoacoustic spectrometer based on a continuous-wave cual-cavity optical parametric oscillator," *Optics Express* **11**, pp. 2820–2825, 2003.
14. K. Schneider, P. Kramper, S. Schiller, and J.Mlynek, "Towards an optical synthesizer:a single-frequency parametric oscillator using periodically poled lithium niobate," *Opt. Lett.* **22**, pp. 1293–1295, 1997.

15. M. van Herpen, S.C.Li, S.E.Bisson, S. te Lintel Hekkert, and F. Harren, "Tuning and stability of a continuous-wave mid-infrared high-power single resonant optical parametric oscillator," *Appl. Phys. B.* **75**, pp. 329–333, 2002.
16. G. Turnbull, D. McGloin, I. Lindsay, M. Ebrahimzadeh, and M. Dunn, "Extended mode-hop-free tuning of a dual-cavity, pump-enhanced optical parametric oscillator," *Opt. Lett.* **25**, pp. 341–343, 2000.
17. D. Kleine, H. Dahnke, W. Urban, P. Hering, and M. Mürtz, "Real-time detection of (CH4)-C-13 in ambient air by use of mid-infrared cavity leak-out spectroscopy," *Opt. Lett.* **25**, pp. 1606–1608, 2000.
18. D. Halmer, G. von Basum, P. Hering, and M. Mürtz, "Fast exponential fitting procedure for real time instrumental use," *Rev. Sci. Instr.* (submitted), 2003.
19. "Hitran2000." Spectral Database, http://www.hitran.com.